EUROPEAN ORGANIZATION FOR NUCLEAR RESEARCH

CERN-EP/90-43
5 April 1990

Single Ionizaton of Helium by 40 to 3000 keV Antiprotons

L.H. Andersen, P. Hvelplund, H. Knudsen, S.P. Moller,
J.O.P. Pedersen, S. Tang-Petersen and E. Uggerhoj

Institute of Physics, University of Aarhus, DK-8000 Aarhus C
Denmark

K. Elsener

CERN, CH-1211 Geneva, Switzerland

E. Morenzoni

PSI, CH-5234 Villigen, Switzerland

Abstract

Measurements of single-ionization cross sections for antiproton impact on helium atoms are reported for impact energies ranging from 40 keV to 3 MeV. It is found that the measured cross sections are in good agreement with recent theoretical estimates based on the continuum-distorted-wave approximation. From a comparison with similar proton data, the ratio between antiproton and proton results is obtained. The energy dependence of this ratio is compared with various theoretical estimates and explained as a result of polarization and binding effects.

(submitted to Phys. Rev. Letters)

Single ionization of various atomic species in collisions with energetic ions is a process which has been investigated intensively during the last 70 years. A new dimension has been added to these investigations by the establishment of low-energy antiproton ($\bar{p}$) beams at the European Organisation for Nuclear Research (CERN). For the first time, we are now able to report on single-ionization measurements of atoms by antiprotons over a broad energy region and to compare with equivelocity proton results.

At high energies, single ionization is well described by the first Born approximation[1], which predicts that the cross section for single ionization scales as q^2, where q is the projectile charge. It is known from measurements with multiply charged ions (He^{2+}, Li^{3+}, etc.)[2] that this q^2 scaling breaks down at low energies. The observed deviation from first-order theories such as the Born approximation can be spelled out in various ways, but an intuitive explanation for the deviation from a q^2 behaviour can be given as follows: At high velocities, where the projectile velocity v_p is much larger than the target electron orbital velocity v_e, a first-order perturbation treatment is valid, and there is no $\bar{p}/p$ difference. At medium energies $v_p \sim v_e$, polarization of the target-electron cloud during the collision plays a role, resulting in an enhancement of the p cross section relative to that of $\bar{p}$. Then at even lower energies, binding effects become important. The binding effect appears as a result of a change in the effective nuclear charge in close-encounter collisions. When a proton is inside the target atom, atomic electrons are subject to increased attraction, while they are subject to reduced attraction when an antiproton is inside the target atom. In the region, where binding dominants, the antiproton cross section is therefore larger than the proton cross section.

The various mechanisms, which influence the $\bar{p}/p$ difference in the cross sections, have been put in a quantitative form in the continuum-distorted-wave eikonal-initial-state calculations by Fainstein et al.[3]. Similar results have been obtained in classical-trajectory Monte-Carlo calculations by Olson[4], Schultz[5] and Ermolaev[6] and by the forced-impulse method of Reading and Ford[7].

The experimental results were obtained with a 5.9 MeV $\bar{p}$ beam extracted from LEAR which was slowed down by passing beryllium, aluminum and mylar foils as well as a thin scintillator before entering the collision region (Fig. 1). The energy of each antiproton was determined by measuring the time-of-flight (TOF) of the antiprotons between the 100 μm thick start scintillator and a 1-mm thick stop scintillator placed ~50 cm downstream.

The time resolution obtained was 2.4 ns (full width at half maximum), corresponding to an energy resolution of 1.2 keV at 50 keV and 300 keV at 2 MeV. A typical TOF spectrum obtained with a degrader foil, which was made inhomogeneous so that a broad energy distribution of exiting $\bar{p}$'s could be obtained, is shown in Fig.2. A detailed description of the calibration procedure and the experimental setup is given in our earlier publications[8,9].

The He^+ ions produced in the target gas cell were accelerated towards a channeltron, and their TOF with respect to the antiproton signals was recorded event by event. For normalization, one out of every thousand antiprotons was selected, and its time of flight was determined. By normalizing the number of counts during a time interval in the antiproton TOF spectrum

corresponding to production of He^+ to the number of counts in the corresponding time interval in the normalization TOF spectrum, we obtained the relative ionization probabilities as a function of antiproton energy.

Since the stop detector has a diameter of 8 cm, only antiprotons, which are deflected less than 4.5^0 in the degrader foil, are counted. This ensures that the size of the degraded beam in the target cell is less than that of the aperture in the time-of-flight tube. It is known from earlier experiments that the target pressure is not uniform in the collision region[8]. This could create problems if the angular distribution of the degraded antiprotons depends strongly on their exit energy. Calculations with the TRIM code[10], however, indicate that such an effect can be ignored under the present experimental conditions.

From our earlier measurements[11], we know that single-ionization cross sections for equivelocity protons and antiprotons agree, as expected on the basis of the first Born approximation at energies above ~1.5 MeV, and we have therefore chosen to normalize our measured relative cross sections to high-energy proton data. We have used the Belfast[12,13] proton data for this normalization and for the following comparison of proton and antiproton data. The Belfast data are chosen because they cover the energy interval between 10 keV and 2.4 MeV which is the energy range of interest in the present experiment. By using data from the same group both for normalization at high energies and for comparison at lower energies, we hope to eliminate errors in the extracted $\bar{p}/p$ cross section differences.

Figure 3 shows our measured cross sections together with the proton cross sections by Shah and Gilbody[12] and Shah et al.[13]. Above ~500 keV, there is no difference between the proton and antiproton results within the experimental uncertainty (~±7%). Note that at the highest energies (~2 MeV), the uncertainty amounts to ~±12% due to a combination of low beam intensity and relatively poor energy resolution. At energies between 50 keV and 500 keV, the proton cross section exceeds that of the antiproton by up to 22%, and at energies below 50 keV, the $\bar{p}/p$ difference is reversed in sign.

Calculated $\bar{p}/p$ cross sections by Fainstein et al.[3] based on the continuum-distorted-wave eikonal-initial-state (CDW-EIS) model are also shown in Fig. 3. It can be seen from the figure that qualitatively, the energy dependent $\bar{p}/p$ difference is well predicted by the model. This means that the description of the influence of polarization at medium energies and of binding at low energies in the model is supported by the present measurements. It should also be noted that on an absolute scale, there is very good agreement between theory and experiment for antiprotons. For medium to low energies the theory for antiprotons is even in better agreement with experiment than the theory for protons.

In order to compare our experimental results to calculated values by various groups, the ratio between total cross sections for single ionization of He by antiprotons to that for protons is shown in Fig. 4. It is seen from the figure that the general behaviour of the ratio between $\bar{p}/p$ cross sections is well described by all the theoretical estimates. The large fluctuations in the ratio $\sigma(\bar{p})/\sigma(p)$ around 2 MeV is caused by large statistical uncertainties in the $\bar{p}$ data due to low beam intensity at these energies.

Reading and Ford[7] estimated the ratio $\sigma(\bar{p})/\sigma(p)$ to be 0.88 at 330 keV and 0.98 at 1 MeV. They used the forced-impulse method with coupled-channel calculations. Olson[4] used classical-trajectory Monte-Carlo (CTMC) calculations and obtained values for the $\sigma(\bar{p})/\sigma(p)$ ratio from 250 keV to 1 MeV. This method was later used by Schultz[5] in the energy interval 6-1200 keV. Recently Ermolaev[6] has used the CTMC method as well as a close-coupled impact-parameter (CCIP) method and has obtained values for the $\sigma(\bar{p})/\sigma(p)$ ratio in the energy interval from 10 keV to 5 MeV.

From the comparison between experimental and theoretical results in Fig.4, it is difficult to give more credit to one model than to the others. A more detailed understanding of the difference in ionization by positive and negative heavy particles must await more elaborate theoretical estimates.

In our earlier work[14] we measured the difference in stopping power S for equivelocity protons and antiprotons, the so-called Barkas effect. It was found that the antiproton stopping power is smaller than the proton stopping power in a silicon target. The Barkas effect has been interpreted as a result of polarization of the target much like the $\bar{p}/p$ difference in ionization mentioned earlier. The Barkas term has been calculated by among others Jackson and McCarthy[15], and based on their results and experimental proton stopping powers in He it is possible also to estimate the antiproton stopping power.

From the present measurements we have estimated the part of the stopping power S_I stemming from ionization events by assuming that the average energy loss in such events is ~80 eV (see Rudd[15]), i.e., $S_I = \sigma \cdot 80$ (eV cm^2/atom). It is found for protons that S_I amounts to about 80% of the total stopping power S in the energy interval from 100 to 500 keV. Using the Jackson-McCarthy[16] theory as a guideline, we find that $S(\bar{p})/S(p)$ for helium is approximately the same as the ratio $S_I(\bar{p})/S_I(p)$ deduced from the present work. This indicates that the 'ionization contribution' of the stopping power contributes to the Barkas effect according to its relative importance in the total stopping power.

It would be interesting to extend the present type of measurements towards even lower energies, where the collision can be described through a quasimolecular model. Kimura and Inokuti[17] have recently suggested that at projectile velocities much smaller than the electron orbital velocity, a dominant ionization process is the so-called adiabatic ionization. In a p+He collision, the electronic binding energy increases with decreasing internuclear distance R. This is in contrast to a $\bar{p}$+He collision, where the electronic binding energy decreases with decreasing internuclear distance. This implies that some portion of the inelastic $\bar{p}$ collisions through avoided crossings between electronic states and the continuum leads to ionization. With respect to Fig. 4, this effect would cause the $\sigma(\bar{p})/\sigma(p)$ ratio to attain very large values at low projectile energies.

Such measurements at antiproton energies below 10 keV are not feasible at present and must await further progress at the LEAR facility[18] towards the production of very low-energy antiproton beams.

One of us (JOPP) would like to acknowledge support from the Carlsberg Foundation.

REFERENCES

1) M.E. Rudd, Y.-K. Kim, D.H. Madison and J.W. Gallagher, Rev. Mod.Phys. 57(1985)965
2) H. Knudsen, L.H. Andersen, P. Hvelplund, G. Astner, H. Cederquist, H. Danared, L. Liljeby and K.-G. Rensfelt, J.Phys.B 17(1984)3545
3) P.D. Fainstein, V.H. Ponce, and R.D. Rivarola, Phys.Rev.A 36 (1987)3639
4) R.E. Olson, Phys.Rev.A 36(1987)1519
5) D.R. Schultz, Phys.Rev.A 40(1989)2330
6) A.M. Ermolaev (private communication)
7) J.F. Reading and A.L. Ford,J. Phys. B 20(1987)3747
8) L.H. Andersen, P. Hvelplund, H. Knudsen, S.P. Møller, A.H. Sørensen, K. Elsener, K.-G. Rensfelt, and E. Uggerhøj, Phys. Rev.A 36(1987)3612
9) L.H. Andersen, P. Hvelplund, H. Knudsen, S.P. Møller, J.O.P. Pedersen, S. Tang-Petersen, E. Uggerhøj, K. Elsener and E. Morenzoni, Phys.Rev. A 40(1989)7336
10) D. Holtkamp (private communication)
11) L.H. Andersen, P. Hvelplund, H. Knudsen, S.P. Møller, K.-G. Rensfelt, and E. Uggerhøj, Phys.Rev.Letters 57(1986)2147
12) M.B. Shah and H. B.Gilbody, J.Phys.B 18(1985)899
13) M.B. Shah, P. McCallion and H.B. Gilbody, J.Phys.B 22(1989) 3037
14) L.H. Andersen, P. Hvelplund, H. Knudsen, S.P. Møller, J.O.P. Pedersen, E. Uggerhøj, K. Elsener, and E. Morenzoni, Phys.Rev.Letters 62(1989)1731
15) M.E. Rudd, Phys.Rev.A 38(1986)6129
16) J.D. Jackson and R.L. McCarthy, Phys.Rev.B 6(1972)4131
17) M. Kimura and M. Inokuti, Phys.Rev.A 38(1988)3801
18) J. Eades and L.M. Simons, Nucl.Instrum.Methods A 278(1989)368

FIGURE CAPTIONS

Fig. 1. Schematic drawing of the experimental setup. The numbers refer to: 1 accelerator facility; 2 time-of-flight tube; 3 channeltron detector; 4 stop detector, 5 start detector, 6 degrader foil.

Fig. 2. TOF spectrum for 5.9-MeV $\bar{p}$ after passage of a 'sandwich' aluminum degrader. The spectrum shows a peak for fast (approx. 2 MeV) $\bar{p}$ and a broader region extending down to the slowest $\bar{p}$ of 40 keV. Background prevents the use of signals at longer flight times, i.e., lower energies.

Fig. 3. Total cross sections for single ionization of He by protons and antiprotons as a function of energy. ●: Present antiproton data; —— proton experimental data, Refs. 12 and 13; —··— and —·—: CDW-EIS theoretical results for antiprotons and protons, respectively, Ref. 3.

Fig. 4. The ratio between total single-ionization cross sections of He for antiprotons and protons $\sigma(\bar{p})/\sigma(p)$ as a function of energy. ●: Present results divided by proton data from Refs. 12 and 13. Theory: o, Ref. 7; Δ, Ref. 4; —·— —, Ref. 3; —··—, Ref. 5; —···—, Ref. 6 (CTMC); — — —, Ref. 6 (CCIP).

FIGURE CAPTIONS

Fig. 1. Schematic drawing of the experimental setup. The numbers refer to: 1 accelerator facility; 2 time-of-flight tube; 3 channeltron detector; 4 stop detector, 5 start detector, 6 degrader foil.

Fig. 2. TOF spectrum for 5.9-MeV $\bar{p}$ after passage of a 'sandwich' aluminum degrader. The spectrum shows a peak for fast (approx. 2 MeV) $\bar{p}$ and a broader region extending down to the slowest $\bar{p}$ of 40 keV. Background prevents the use of signals at longer flight times, i.e., lower energies.

Fig. 3. Total cross sections for single ionization of He by protons and antiprotons as a function of energy. •: Present antiproton data; —— proton experimental data, Refs. 12 and 13; —··— and —·—: CDW-EIS theoretical results for antiprotons and protons, respectively, Ref. 3.

Fig. 4. The ratio between total single-ionization cross sections of He for antiprotons and protons $\sigma(\bar{p})/\sigma(p)$ as a function of energy. •: Present results divided by proton data from Refs. 12 and 13. Theory: o, Ref. 7; Δ, Ref. 4; —·— —, Ref. 3; —··—, Ref. 5; —···—, Ref. 6 (CTMC); — — —, Ref. 6 (CCIP).

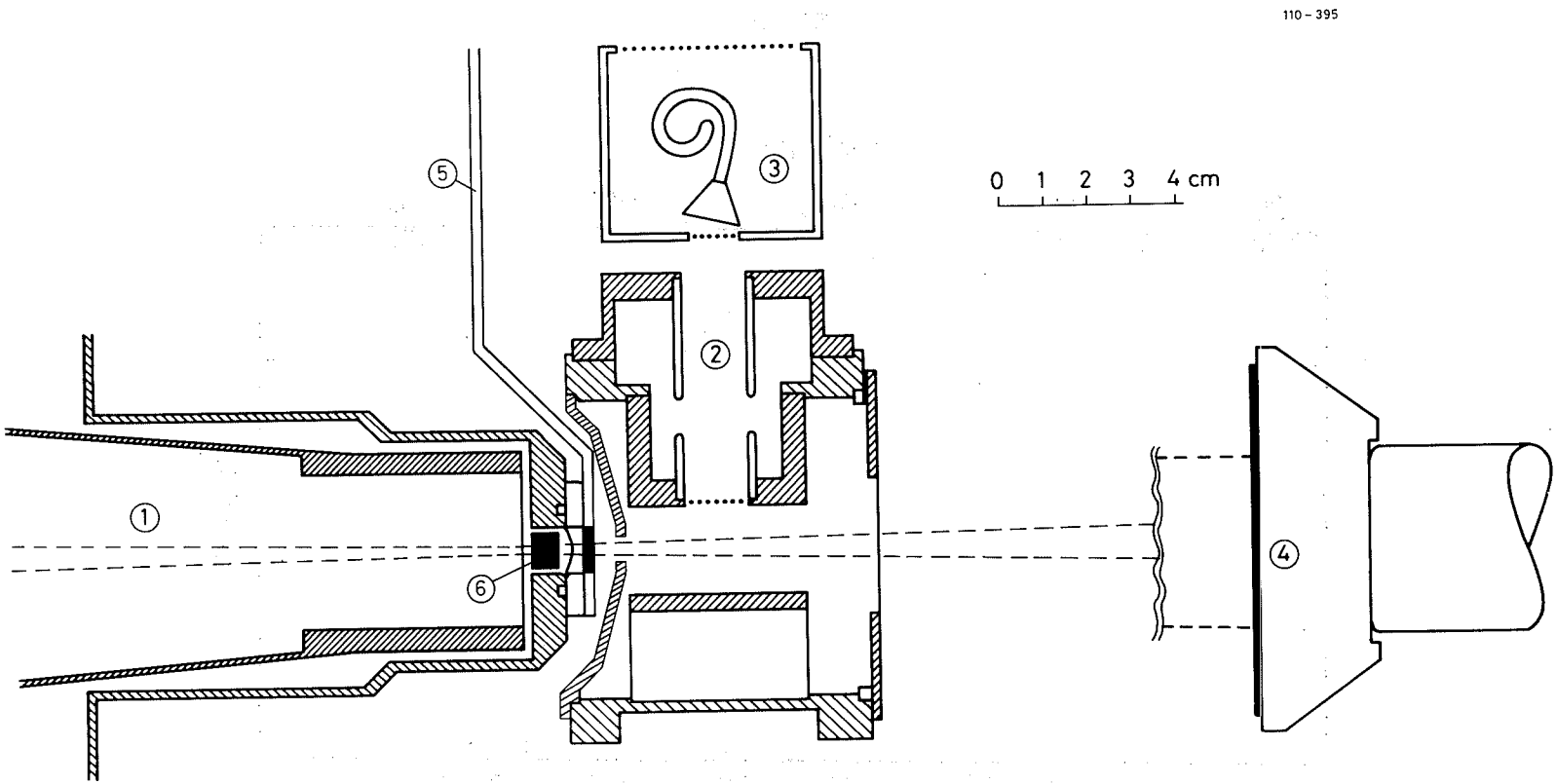

Fig.1

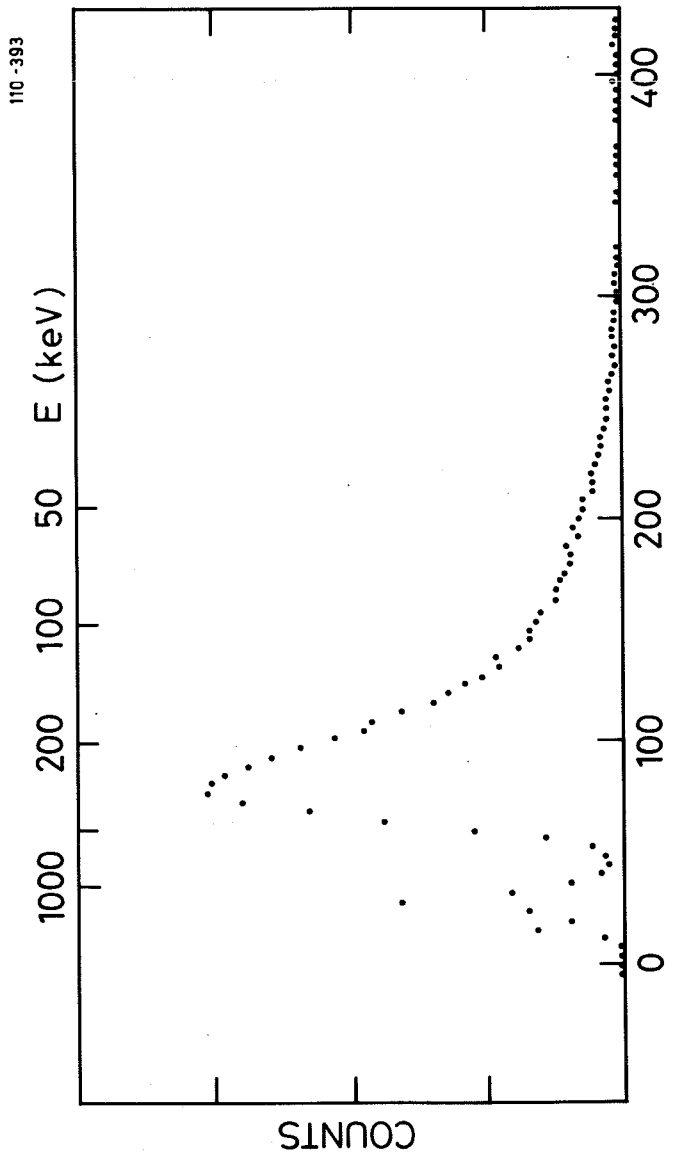

Fig.2

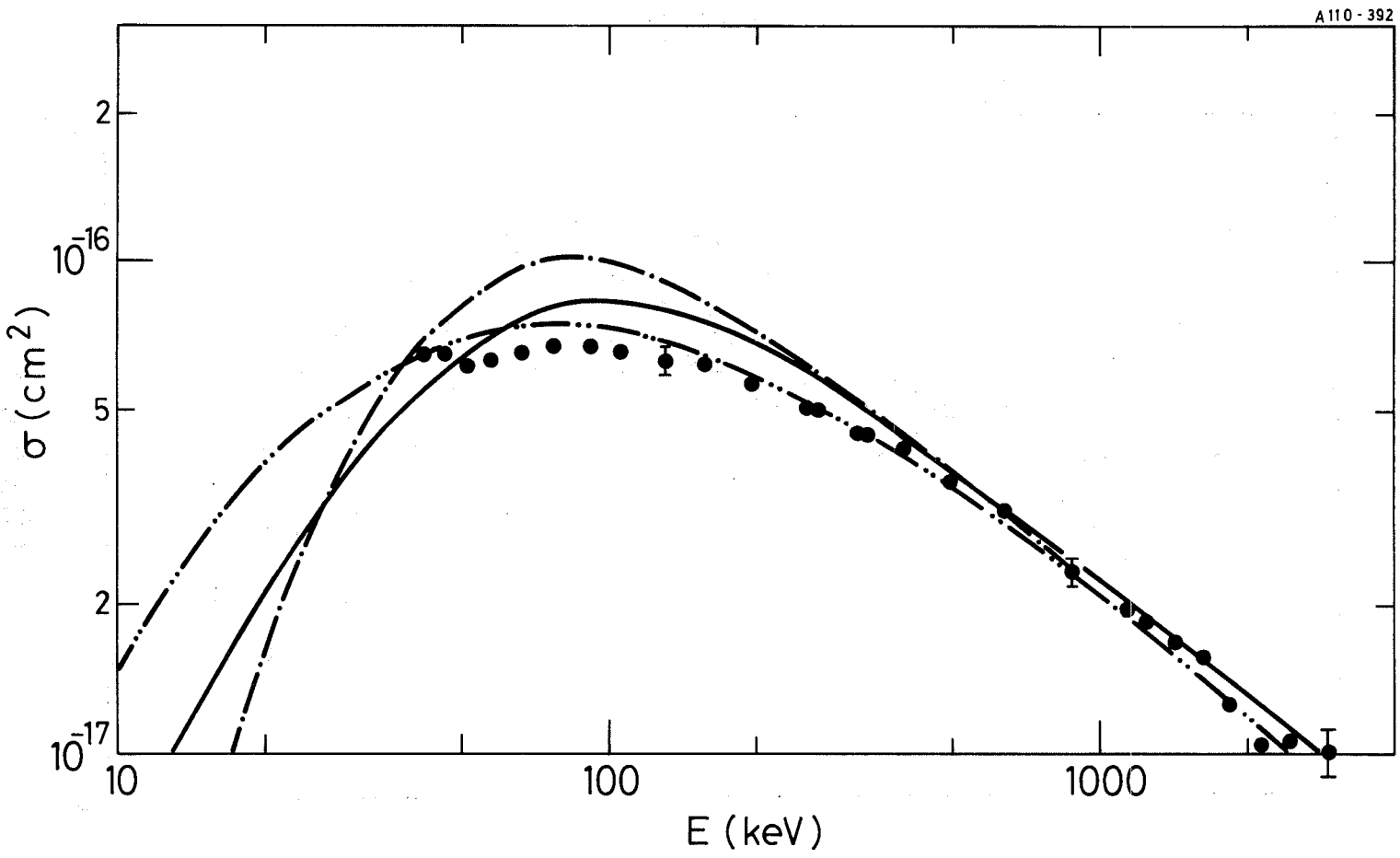

Fig.3

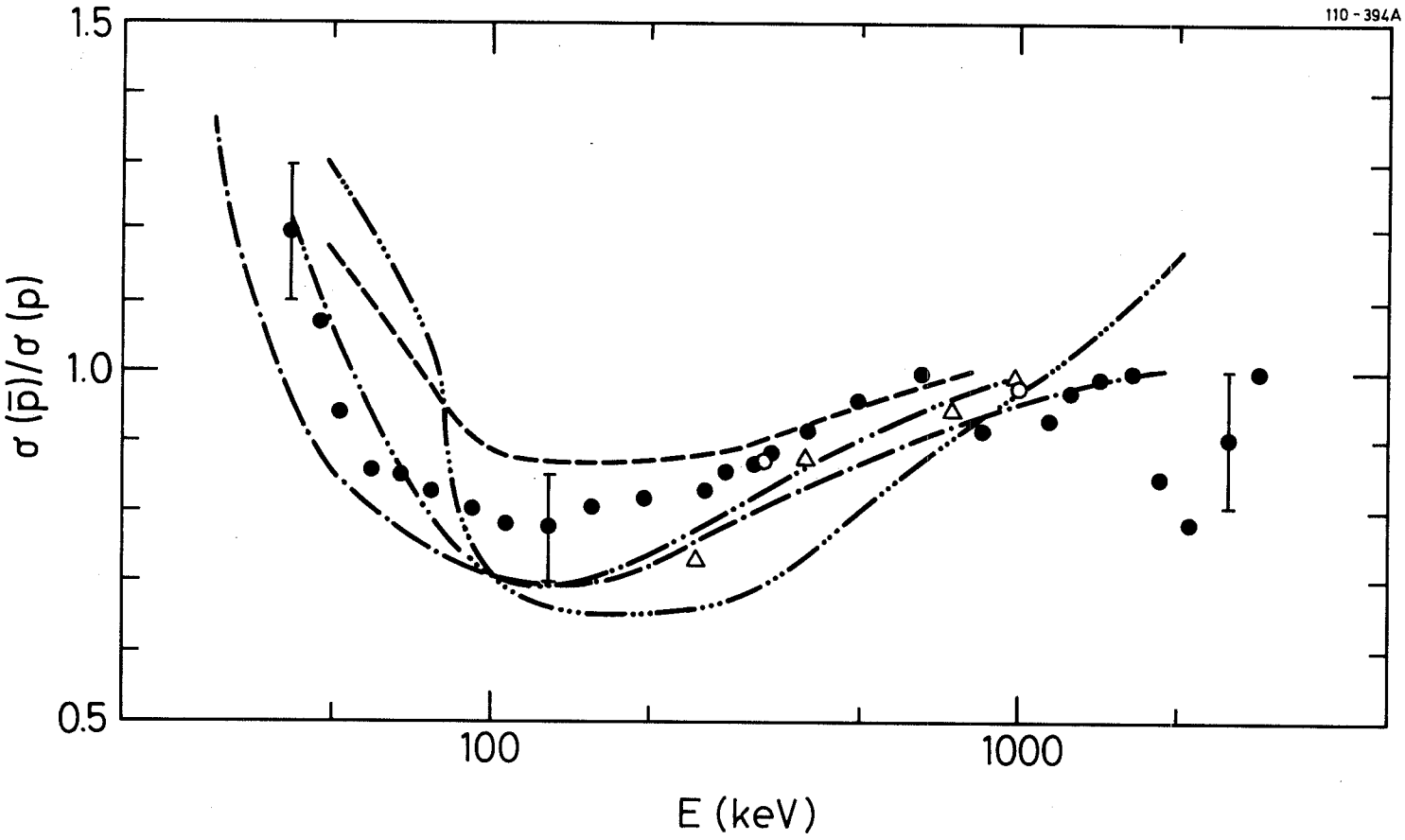

Fig. 4